

Electrorotation of Erythrocytes Treated with Dipicrylamine: Mobile Charges within the Membrane Show their “Signature” in Rotational Spectra

V.L. Sukhorukov, U. Zimmermann

Lehrstuhl für Biotechnologie der Universität Würzburg, Am Hubland, D-97074 Würzburg, Germany

Received: 14 February 1996/Revised: 29 May 1996

Abstract. In this study, electrorotation spectra of individual cells (that is, frequency dependence of cell rotation speed) have been proved to yield information not only about the passive electric properties of cell constituents, but also about the presence of mobile charges within the plasma membrane being part of ion carrier transport systems. Experiments on human erythrocytes pretreated with the lipophilic anion dipicrylamine (DPA) gave convincing evidence that these artificial mobile charges adsorbed to the plasma membrane contributed significantly to the rotational spectrum at relatively low conductivity of the external medium ($2\text{--}5\text{ mS m}^{-1}$). Theoretical integration of the mobile charge concept into the single-shell model (viewing the cell as a homogenous sphere surrounded by a membrane) led to a set of equations which predicted electrorotational behavior of DPA-treated cells in dependence on medium conductivity. The quantitative data on the partition and the transmembrane translocation rate of the DPA anion extracted from the experimental rotational spectra agreed well with the corresponding literature values.

Key words: Mobile charges — Dielectric Spectroscopy — Electrorotation — Dispersion — Membrane Capacity — Membrane Conductivity — Lipophilic Ion

Introduction

Electrorotation of single cells (and organelles) in a rotating field has yielded useful data on membrane properties and other parameters (Arnold & Zimmermann, 1982; Jones, 1995; Fuhr, Zimmermann & Shirley, 1996). Electrorotation has also proved useful in gathering statistically significant data on cell populations (Arnold &

Zimmermann, 1988; Sukhorukov et al., 1994, 1995; Fuhr et al., 1996). The implementation of this technique is simple. The particle rotation speed is measured as a function of the frequency, usually with the electric field strength fixed. The main features of electrorotation for biological cells are fairly well understood. At low frequencies (kHz range), a cell has a very large apparent permittivity arising mainly from membrane charging. Theory suggests strong antifield rotation, and this is, in fact, found experimentally. Treatment of cells with membrane-destructive agents will abolish or even reverse this rotation (Arnold et al., 1988), indicating that plasma-membrane charging is the dominant mechanism of polarization in the kHz-range. At high frequencies (MHz range), the reactance of the membranes becomes negligible and the cell conductivity essentially becomes equal to the cytoplasmic conductivity (Fuhr et al., 1996). Cofield rotation occurs provided the cytosolic conductivity exceeds that of the external medium. This demonstrates that a living cell cannot be modeled by assuming a homogeneous sphere, because only one electrorotation peak is expected (Jones, 1995). Therefore, the rotational behavior of a living cell is usually explained by modeling a cell as a homogeneous, nondispersive spherical particle surrounded by a very thin shell corresponding to the membrane. However, in many cases, it can be shown that rotational spectra (that is, rotation speed *vs* frequency at fixed voltage) cannot be fitted accurately on the basis of this single-shell model. One reason for this could be that a cell contains liquid, viscous and solid components, and membrane-bound compartments that can contribute to the rotational spectra. In principle, such complex rotational spectra can be described by the introduction of more shells. A general problem with these multiple-shell models is that the number of unknowns is too large to allow unambiguous values to be assigned to any of them.

Another reason for the occurrence of dielectric

“anomalies” in rotational spectra has not yet been considered quantitatively in current theories: the electrical properties of the membrane itself may be frequency dependent. Such a dependence is—among other things (Arnold & Zimmermann, 1988)—expected if the membranes contain high concentrations of mobile charges being involved in ion carrier systems (Zimmermann, Büchner & Benz, 1982; Wang et al., 1991; Wang, Zimmermann & Benz, 1994). Mobile charges can lead to dielectric dispersion of the plasma membrane capacitance (and conductance) in the kHz range (Läuger et al., 1981). In agreement with this assumption, charge-pulse experiments on planar lipid bilayer membranes (Benz & Läuger, 1977; Benz & Zimmermann, 1983; Dilger & Benz, 1985) and on nerve membranes (Benz & Conti, 1981; Benz & Nonner, 1981; Benz, Conti & Fioravanti, 1984) have shown that the incorporation of artificial mobile anions, such as dipicrylamine (DPA), into the membranes led (in addition to the membrane resistance/capacitance-relaxation) to the occurrence of a second exponential relaxation curve during the discharging process. Accordingly, the apparent specific capacitance of the membranes in the presence of these lipophilic anions was 5–10 times higher than the geometrical specific capacitance.

In this study, we have performed electrorotation experiments on human erythrocytes both in the presence and absence of DPA. For untreated cells, the best agreement with theory and experiment (despite the biconcave shape and an electrogenic $\text{Na}^+\text{-K}^+\text{-ATPase}$) could be obtained by using the single-shell spherical model (as in the case of impedance measurements) (*see* literature quoted in Fuhr et al., 1996). In contrast, the rotational spectrum of DPA-treated cells could be fitted quite accurately only if the frequency-dependent capacitive and conductive contribution of the lipophilic anions in the kHz-range were integrated into the equations of the single-shell model. The translocation rate and the area-specific concentration of the DPA molecules within the membrane extracted from the rotation experiments agreed well with the corresponding data derived from the charge pulse experiments mentioned above.

Materials and Methods

CELLS

Human heparinized blood samples were withdrawn from apparently healthy donors and used on the day of collection for rotation measurements. After centrifugation ($600 \times g$, 5 min) the buffy coat and the plasma were removed. Then the erythrocytes were washed twice in isotonic phosphate buffer saline (PBS), containing 137 mM NaCl, 2.6 mM Na_2HPO_4 , 1.5 mM KH_2PO_4 , pH 7.3.

ELECTROROTATION EXPERIMENTALS

Before electrorotation, the cells were washed 2–3 times with 280-mOsm inositol solutions (Sigma, I-5125). After resuspension of the

cell pellet in inositol solution (at a final suspension density of 10^5 cells ml^{-1}) the conductivity was adjusted ($1\text{--}20$ mS m^{-1}) by addition of appropriate amounts of a 0.2 M HEPES-KOH solution (pH 7.3). Conductivity and osmolality of the solutions were measured by means of a digital conductometer (Knick GmbH, Berlin) and a cryoscopic osmometer (Osmomat 030, Gonotec GmbH, Berlin), respectively. The viscosity of the solutions was determined to be 1.05 mPa sec according to the method described elsewhere (Sukhorukov, Arnold & Zimmermann, 1993). DPA (2,2',4,4',6,6'-hexanitrodiphenylamine, Fluka, Basel, Switzerland) was added to the solution at a final concentration of 1–10 μM from an ethanol stock solution. The concentration of DPA was determined spectrophotometrically (Perkin-Elmer Lambda 2 UV/VIS, Beaconsfield, Buckinghamshire, UK) using a molar extinction coefficient of $\epsilon_{412} = 2.6 \times 10^4$ $\text{M}^{-1} \text{cm}^{-1}$ (Wulf, Benz & Pohl, 1977).

About 10 μl of the suspension (containing on average 10^3 cells) were pipetted into the macroscopic four-electrode chamber which had been described in detail by (Arnold & Zimmermann, 1989). The spacing of the planar electrodes (mounted at right angles to each other) was about 1.4 mm. Two opposite electrodes were connected to a conductometer to allow solution conductivity to be monitored. The electrodes were driven by four 90° phase-shifted square wave voltages (1:1 mark:space) of 13.7 V amplitude¹ using a pulse generator developed by G. Fuhr (Humboldt-University, Berlin, Germany).

In one set of experiments, the characteristic frequency (f_{c1}) of the antifield rotation peak in dependence on medium conductivity was determined by using the “null-frequency” (i.e., the contrarotating field) technique described in detail by Arnold & Zimmermann (1983).

The electrorotation chamber was covered with a microslide and viewed with a Leica Fluolux inverted microscope and a $100 \times$ oil-immersion objective. The microscope was equipped with a LCD video camera connected to a videotape recorder. Rotation spectra were monitored over the frequency range 500 Hz to 15 MHz. Rotation data of cells were only used for evaluation which were positioned close to the center of the chamber (far away from other cells and from the electrodes). The rotation spectra were fitted on the basis of the single-shell or mobile charge model (*see below*) using the *Mathematica*[®] software developed by Wolfram (1991).

Theoretical Considerations

SINGLE-SHELL MODEL

Many field-induced effects have frequency dependencies which are determined by the effective polarizability of the particle. In a liquid medium, this is dependent on the properties of the medium as well as the particle: the appropriate expression is usually referred to as the Clausius-Mosotti factor (U). This is extended from the usual purely dielectric expression to give a complex factor U^* which we may define in terms of the admittance ($\sigma^* = \sigma + j\omega\epsilon_o\epsilon$) as:

$$U^* \equiv (\sigma_p^* - \sigma_e^*) / (\sigma_p^* + 2\sigma_e^*) \quad (1)$$

¹ Because the local field strength (and the frictional force experienced by an individual cell) is poorly characterized, the data were corrected by the so-called scaling factor as described by Gascoyne, Becker & Wang (1995).

where σ is the conductivity (real), ϵ is the relative permittivity (real), ϵ_o is the permittivity of vacuum, ω is the angular frequency and $j \equiv \sqrt{-1}$; the subscript “ e ” refers to the medium and subscript “ p ” refers to the particle, viewed as a homogeneous sphere. The real part of U^* determines the dielectrophoretic force on a particle, while in the case of electrorotation it is the imaginary part (U'') that we must consider. If U'' is known, the torque L experienced by the particle can be calculated from:

$$L = -4\pi\epsilon_o\epsilon_e a^3 E^2 U'' \quad (2)$$

where a is the radius of the particle and E is the field strength of the rotating field. Substitution of the viscous resistance experienced by a rotating sphere shows that the steady-state rotation speed (Ω) is given by:

$$\Omega = -\epsilon_o\epsilon_e E^2 U'' / 2\eta \quad (3)$$

where η is the viscosity of the medium.

In the single-shell model, a cell is approximated by a homogeneous, conductive sphere of radius (a) surrounded by a shell of thickness (d), corresponding to the membrane (subscript “ m ”). For such a single-shell particle, σ_p^* is given by Eq. 4 (Pauly & Schwan, 1959):

$$\sigma_p^* = \sigma_m^* \frac{\sigma_m^* + (1/3)(\sigma_i^* - \sigma_m^*)(1 + 2\nu^3)}{\sigma_m^* + (1/3)(\sigma_i^* - \sigma_m^*)(1 - \nu^3)} \quad (4)$$

where $\nu = a/(a + d)$, and σ_i^* is the admittance of the cytosol. For the case of $d \ll a$, Eq. 4 simplifies to Eq. 5

$$\sigma_p^* = G_m^* \frac{a \cdot \sigma_i^*}{a \cdot G_m^* + \sigma_i^*} \quad (5)$$

where G_m^* is the membrane admittance (complex conductivity per unit area) given by:

$$G_m^* = G_m + j\omega C_m \quad (6)$$

where $C_m = \epsilon_m \cdot \epsilon_o / d$ and $G_m = \sigma_m / d$ are the area specific membrane capacitance ($F m^{-2}$) and conductance ($S m^{-2}$), respectively. Combination of Eqs. 5 and 6 with Eq. 1 and substitution of U'' in Eq. 3 yield the equation for the rotation speed (Ω) of a cell.

The theoretical plots of Ω in dependence on frequency are depicted in Fig. 1. The curves were calculated for different external conductivities (σ_e) using appropriate data for the cell and membrane parameters. It is evident from Fig. 1, that the characteristic frequency of the antifield rotation peak (f_{c1}) is shifted towards higher frequencies with increasing conductivity of the solution. The single-shell theory shows for low-conductivity solutions, that the conductivity-dependence

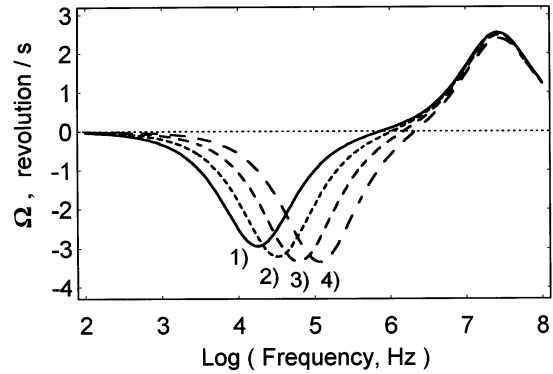


Fig. 1. Rotational spectra of cells calculated theoretically on the basis of the single-shell model (by using Eqs. 1, 3, 5 and 6) for various medium conductivities, σ_e (curves 1–4: 1, 2, 4 and 8 $mS m^{-1}$, respectively). For calculation of the spectra the following parameters were used: radius 4 μm , area-specific (passive) membrane capacitance (C_m) 5 $mF m^{-2}$, area-specific (passive) membrane conductance (G_m) 100 $S m^{-2}$, internal conductivity (σ_i) 0.3 $S m^{-1}$, relative dielectric constant of the cytoplasm (ϵ_i) 50 and of the aqueous medium (ϵ_e) 80; the field strength, $E = 9.8 kV m^{-1}$, the viscosity of the 280 mOsm inositol, $\eta = 1.05 mPa s$.

of f_{c1} (normalized to the radius, a) is given by (Arnold & Zimmermann, 1988; Fuhr et al., 1996):

$$f_{c1} a = \sigma_e / (\pi C_m) + a G_m / (2\pi C_m) \quad (7)$$

The characteristic frequency, f_{c1} , can be measured highly accurately by using the “null-frequency” method (see above), provided that the rotational spectrum can be fitted on the basis of the single-shell model.

MOBILE CHARGE MODEL

The presence of mobile charges within the membrane has not been considered in the single-shell model yet. Ketterer, Neumcke & Lauger (1971) showed that the transport of a lipophilic ion (such as DPA) through bilayer membranes occurs in three elementary steps: (1) the adsorption of the ion to the membrane-solution interface; (2) the translocation of the ion across an energy barrier to the opposite membrane interface; and (3) desorption from the interface into the aqueous solution (for review see Lauger et al., 1981).

The analytical expressions for the admittance (or the impedance) and for the dielectric loss factor of a membrane doped with lipophilic ions were derived by Ketterer et al. (1971). The mathematical analysis of these authors (see Eqs. 53 and 54 in Ketterer et al., 1971) have demonstrated that the membrane admittance is determined by the area-specific concentration of the mobile charges and their translocation rate constants. The general equations derived by Ketterer et al. (1971) can be simplified if we take into account that for most lipophilic

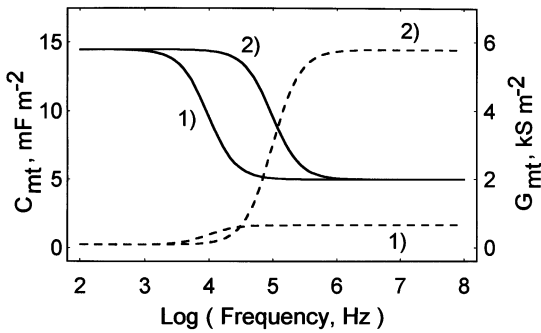


Fig. 2. Frequency-dependence of the total membrane capacitance, C_{mt} (solid lines) and conductance, G_{mt} (broken lines), predicted theoretically on the basis of the mobile charge model (Eqs. 8 and 9). The dispersion curves were calculated by assuming for the (geometric) dielectric properties of the membrane $C_m = 5 \text{ mF m}^{-2}$ and $G_m = 100 \text{ S m}^{-2}$, and for the area-specific concentration (N) and the translocation rate (k_i) of the mobile DPA charges 5 nmol m^{-2} , $3 \times 10^4 \text{ sec}^{-1}$ (curves 1) and $3 \times 10^5 \text{ sec}^{-1}$ (curves 2), respectively. For further explanation, see text.

ions the adsorption/desorption processes and/or aqueous diffusion are slow compared to their translocation rate within the membrane (Benz, Lauser & Janko, 1976). Taking advantage of this, the following equations can be derived:

$$C_{mc} = (F^2 N / 2RT) (1 / (1 + \omega^2 \tau^2)) \quad (8)$$

and

$$G_{mc} = (F^2 N / 2RT) (\omega^2 \tau / (1 + \omega^2 \tau^2)) \quad (9)$$

where C_{mc} is the capacitance (corresponding to the imaginary part of the admittance) and G_{mc} is the conductance (corresponding to the real part of the admittance) of the mobile charges; F is the Faraday constant, N is the area specific concentration of the mobile charges within the membrane, R is the gas constant and T is the temperature; τ is the time constant of the electric dispersion arising from the mobile charges. The time constant is given by $\tau = 1/2k_i$, provided that symmetric ion conditions on both sides of the membrane are assumed.

Using Eqs. 8 and 9 the frequency-dependence of the total capacitance, $C_{mt} (= C_m + C_{mc})$ and conductance, $G_{mt} (= G_m + G_{mc})$ can be calculated (Fig. 2) by assuming $C_m = 5 \text{ mF m}^{-2}$, $G_m = 100 \text{ S m}^{-2}$, $N = 5 \text{ nmol m}^{-2}$, and $k_i = 3 \times 10^4 \text{ sec}^{-1}$ (Fig. 2, curves 1) and $3 \times 10^5 \text{ sec}^{-1}$ (Fig. 2, curves 2). It is evident from Fig. 2 that a dispersion occurs in the kHz-range when the frequency is close to the reciprocal of the time constant τ . At fixed concentration of the mobile charges, the dispersion is shifted with increasing translocation rate towards higher frequencies. For frequencies $\omega \ll 1/\tau$, the capacitance value is dominated by $C_{mc} = F^2 N / 2RT$, whereas at high field frequencies $\omega \gg 1/\tau$, $C_{mc} = 0$. In contrast, G_{mc}

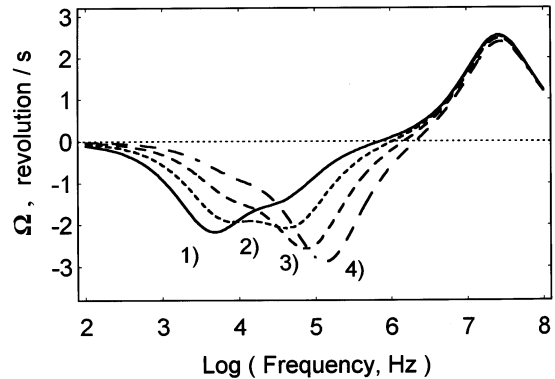


Fig. 3. Rotational spectra of DPA-treated human erythrocytes calculated theoretically on the basis of the mobile charge model (by using Eqs. 3, 5 and 10, and assuming $N = 5 \text{ nmol m}^{-2}$ and $k_i = 3 \times 10^4 \text{ sec}^{-1}$ for various external conductivities σ_e (corresponding to those in Fig. 1). The other parameters were selected as described in Fig. 1.

dominates the total area-specific conductance at frequencies above the dispersion, whereas at low frequencies its contribution is negligible.

Taking into account the total capacitance and conductance, Eq. 6 can be rewritten as:

$$G_{mt}^* = (G_m + G_{mc}) + j\omega(C_m + C_{mc}) \quad (10)$$

After replacement of G_{mt}^* in Eq. 5 by G_{mt}^* , the theoretical rotational spectra for cells containing membranes with integrated mobile charges can be calculated in dependence on the external conductivity, σ_e by using Eqs. 1, 3, 5 and 10, and the above values for C_m , G_m , N and k_i (Fig. 3).

It is evident from Fig. 3 that due to the mobile charges an additional antifield rotation ‘‘shoulder’’ occurs which succeeds in low-conductivity solution (curve 1, $\sigma_e = 1 \text{ mS m}^{-1}$) or precedes (curves 3 and 4, $\sigma_e = 4 \text{ mS m}^{-1}$ and 8 mS m^{-1} , respectively) the major ‘‘antifield rotation peak’’ in conductive solutions. At the intermediate conductivity (curve 2, $\sigma_e = 2 \text{ mS m}^{-1}$), two peaks of approximately equal magnitude are seen. At relatively high conductivities (curve 4, $\sigma_e = 8 \text{ mS m}^{-1}$), the contribution of the mobile charges to the rotational spectrum becomes too small to be resolved: the spectrum resembled that of the single-shell model in the absence of mobile charges (curve 4 in Fig. 1). As expected, the cofield rotation peak (generated by polarization of the cytosol) is not affected by the presence of the mobile charges within the membrane.

RESULTS

Figure 4 shows typical electrorotation spectra for unmodified erythrocytes recorded at various external conductivities. In agreement with the literature (Engel, Do-

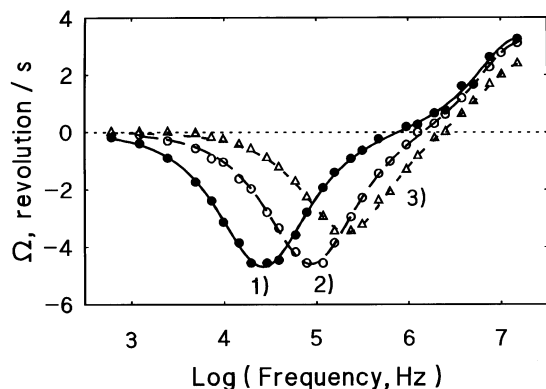


Fig. 4. Rotational spectra of untreated human erythrocytes determined experimentally at medium conductivities of 1 (curve 1), 5.5 (curve 2) and 16.2 (curve 3) mS m^{-1} . The curves were fitted on the basis of the single-shell model by using values for the various parameters given in Table 1.

nath & Gimsa, 1988; Gimsa et al., 1994; Becker et al., 1995), the rotational spectra could be fitted quite accurately on the basis of a single-shell sphere (Eqs. 1, 3, 5, and 6) by selecting appropriate values for various parameters listed in Table 1. The cofield peak could not always be resolved completely due to limitation of the frequency range of the generator. As predicted by the theory (Eq. 7) the characteristic antifield rotation peak (f_{c1}) is shifted towards higher frequencies in response to an increase in the external conductivity, σ_e .

From the spectra the geometric, area-specific capacitance (C_m) was estimated to be on average 6.1 mF m^{-2} . The value was apparently independent of the external conductivity (Table 1). A higher C_m value was obtained by measuring the radius-normalized f_{c1} frequency in dependence on the external conductivity (Eq. 7), using the “null-frequency” method (Fig. 5). From the slope and the ordinate intercept of the highly linear plot (Fig. 5, open symbols), C_m and G_m were calculated (using Eq. 7) to be 8 mF m^{-2} and 260 S m^{-2} , respectively.²

The average value of the internal conductivity (σ_i) deduced from the fitting procedure was smaller (see Table 1) than the values reported in the literature (Becker et al., 1995). This is expected, because it is well known that ion leakage from erythrocytes is enhanced when

² Determination of C_m and particularly of G_m is usually subjected to statistical (and experimental) uncertainties. There are several difficulties associated with the measurement of these parameters that are not unique to rotation; the causes and effects are the same for all techniques that use external fields to induce membrane potentials (for details, see Fuhr et al., 1996). However, it should be noted that the G_m values obtained here were in the range found by other authors for the erythrocyte plasma membrane (0 to 1000 S m^{-2} , Gimsa et al., 1994; $750\text{--}1200 \text{ S m}^{-2}$, Engel et al., 1988).

Table 1. Cellular and membrane parameters of untreated human erythrocytes extracted from the electrorotation spectra using the single-shell model

Cell/ Donor	a μm	σ_e mS m^{-1}	C_m mF m^{-2}	G_m S m^{-2}	σ_i S m^{-1}
K01/VS	3.4	1.2	5.5	50	0.13
K03/VS	3.9	4.2	7.2	400	0.07
K04/VS	3.9	4.2	5.3	200	0.14
K05/VS	4.0	16.0	7.1	1000	0.13
K06/VS	4.0	16.5	5.7	50	0.11
K07/VS	3.9	16.0	6.4	900	0.08
K09/WB	3.2	2.0	5.7	100	0.22
K10/WB	3.3	16.5	6.3	500	0.17
K11/WB	3.4	16.5	6.0	550	0.09
K12/WB	3.3	5.7	6.2	200	0.21
K13/WB	3.2	5.7	5.7	50	0.18
K14/WB	3.5	1.6	5.5	50	0.15
Mean \pm SD	3.6 ± 0.3		6.1 ± 0.6	340 ± 340	0.14 ± 0.05

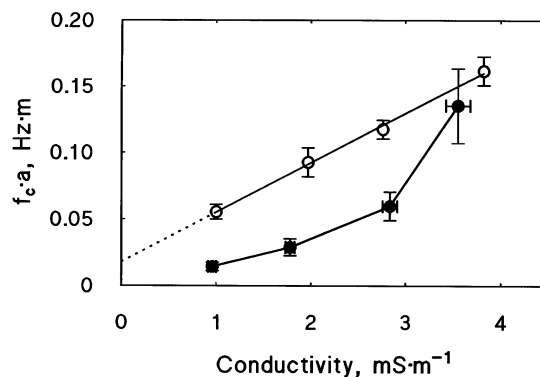


Fig. 5. The characteristic antifield rotation frequency normalized against the radius ($f_c a$) of untreated (open circles) and DPA-treated ($5 \mu\text{M}$, filled circles) erythrocytes in dependence on the medium conductivity, σ_e .

these cells are exposed to extremely low-salinity solutions (Donlon & Rothstein, 1969).

Typical rotational spectra of erythrocytes after treatment with 5 and $10 \mu\text{M}$ DPA are depicted in Fig. 6. Comparison of the rotational spectra with those of the control cells (Fig. 4) shows that the antifield rotation speed of the DPA-treated cells is reduced over the whole frequency range. Simultaneously, the cofield rotation peak is shifted to lower frequencies. The latter effect is expected if DPA is somewhat toxic to the membrane resulting in an (unspecific) increase of the permeability and the apparent conductance of the membrane (see below).

These indirect effects of DPA on the membrane properties must be clearly distinguished from the effects arising from the mobile charges. As illustrated in Fig. 6, treatment of the cells with DPA resulted in dramatic,

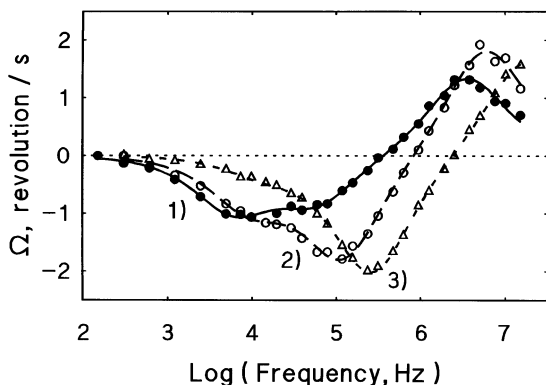


Fig. 6. Typical rotational spectra of erythrocytes measured experimentally on erythrocytes pretreated with 5 (triangles and filled circles) and 10 μM DPA (open circles). The spectra were recorded at three different medium conductivities: (1) 2.0 mS m^{-1} , (2) 5.2 mS m^{-1} and (3) 15.2 mS m^{-1} . The curves were fitted on the basis of the mobile charge model by using values for the various parameters as given in Table 2 (cells D29, D41 and D34).

conductivity-dependent changes of the antifield rotation part of the spectrum. In contrast to Fig. 4, the rotational spectra of DPA-treated cells could not be fitted on the basis of the single-shell model (*fits are not shown*). This can also be seen from the plot of the radius-normalized frequency (f_{c1}) of the “antifield rotation peak” vs. the external conductivity (Fig. 5, filled symbols). It is evident that the increase of the medium conductivity led at some stage to a disproportionate increase in f_{c1} , which cannot be explained by the single-shell model (Eq. 7). The least-square fit of Eq. 7 (*not shown in Fig. 5*) to the data points recorded at conductivities lower than 3 mS m^{-1} yielded an apparent C_m of about 15–20 mF m^{-2} . A similar C_m -value could be extracted from the major “antifield rotation peak” of rotational spectra measured in low-conductivity solution (e.g., curve 1 in Fig. 6). In contrast, evaluation of the rotation spectra performed in solutions of higher conductivities (e.g., curves 2 and 3 in Fig. 6) or analysis of the uppermost part of the ($f_{c1} a$)/ σ_e -plot in Fig. 5 (filled circles) yielded a C_m -estimate of 5–8 mF m^{-2} (by using Eq. 7 after simplification) which is comparable to that found for the untreated erythrocytes.

The apparent increase of the area-specific capacitance in DPA-treated cells at external conductivities lower than 3 mS m^{-1} is a clear indication that DPA showed their signature in the rotational spectrum. In fact, as shown in Fig. 6 an excellent agreement with theory and experiment is achieved, when the experimental rotation spectra were fitted on the basis of the mobile charge model according to Eqs. 1, 3, 5 and 10 (assuming values for the various membrane parameters listed in Table 2). It is obvious that the changes of the position of the antifield peaks and/or shoulders in the frequency spectrum with the increase of medium conductivity

agreed with the theoretical predictions of the frequency-dependence of the capacitive (C_{mc}) and conductive part (G_{mc}) of the mobile charges (*see also Fig. 2*). The analysis showed that in low-conductivity solutions, the antifield rotation peak is dominated by the capacitive properties of the mobile charges, whereas towards higher conductivities, the antifield rotation behavior of the cells is determined by the geometric capacitive properties of the membrane (*see above and Fig. 3*). From experimental curves such as shown in Fig. 6, the value for the geometric (passive) membrane capacitance (C_m) is found to be 5.0–6.0 mF m^{-2} (Table 2) indicating that this parameter had not been changed significantly by the DPA treatment as expected. In the presence of 5 μM DPA, the translocation rate (k_i) and the area-specific concentration (N) of the mobile charges were estimated to be $(3.1 \pm 0.9) \cdot 10^4 \text{ sec}^{-1}$ and $6.1 \pm 1.3 \text{ nmol m}^{-2}$, respectively (*see Table 2*). The values of C_m and k_i were independent of the DPA-concentration (1–10 μM) within the limits of accuracy, whereas the concentration of the mobile charges within the membrane increased and the internal conductivity decreased with increasing DPA-concentration (*see Table 2*). The values of G_m varied statistically between 50 and 900 S m^{-2} .

Discussion

In the last few years, electrorotation has become the principal means used for the dielectric characterization of individual small cells (Arnold & Zimmermann, 1988; Jones, 1995; Fuhr et al., 1996). As shown here, rotational spectra can be analyzed to estimate internal conductivity, membrane capacitance and conductance, and to monitor changes in these properties when cells are subjected to low concentrations of membrane “destructive” agents or other protocols. The relevant data can be extracted from the measurements of the rotation speed and of the frequency dependence of the anti- or cofield rotational motion of the cells.

The magnitude of the rotation speed (at fixed voltage and viscosity) reflect the conductance (and permeability state) of the membrane (Arnold & Zimmermann, 1988). The reduction in the rotation speed observed after incorporation of DPA into the erythrocyte membrane is, therefore, an indication of an increase in the apparent membrane conductivity (G_{mi}).

An increase of membrane permeability in DPA-treated cells is also suggested by the observation that cofield rotation occurs at lower frequencies than in the control cells (Fig. 4 and 6). The frequency range, in which cells exhibit cofield rotation, depends on the internal conductivity (in relation to the external conductivity) (Arnold & Zimmermann, 1988). Therefore, ion loss from the cells due to an increased passive permeability of the membrane will shift the cofield rotation peak to

Table 2. Cellular and membrane parameters of DPA-treated human erythrocytes extracted from the electrorotation spectra using the mobile charges model

Cell/ Donor	a μm	σ_e mS m^{-1}	C_m mF m^{-2}	G_m S m^{-2}	σ_i S m^{-1}	C_{DPA} μM	N nmol m^{-2}	k_i msec^{-1}
D22/WB	3.3	1.5	5.7	100	0.20	1	2.9	19
D38/WB	3.6	7.6	5.0	500	0.12	1	3.0	36
D40/WB	3.7	14.5	5.0	300	0.12	1	1.5	35
D42/WB	3.4	1.2	5.5	100	0.18	1	2.9	27
Mean \pm SD	3.5 ± 0.2		5.3 ± 0.4	250 ± 190	0.16 ± 0.04		2.6 ± 0.7	29 ± 8
D05/VS	3.9	4.5	5.5	300	0.11	5	5.8	32
D06/VS	3.9	4.5	5.5	300	0.08	5	7.6	31
D07/VS	3.7	16.0	5.3	600	0.17	5	5.9	35
D24/WB	3.6	12.5	5.3	400	0.10	5	4.2	51
D25/WB	3.6	6.3	5.0	400	0.08	5	4.0	44
D29/WB	4.1	2.0	5.0	100	0.04	5	5.7	32
D34/WB	3.3	15.2	5.5	200	0.16	5	7.5	35
D35/WB	3.9	6.4	5.0	700	0.08	5	7.0	31
D36/WB	3.9	2.0	5.0	350	0.04	5	4.9	31
D43/WB	4.0	2.0	5.0	100	0.06	5	5.6	20
D44/WB	2.9	1.4	5.2	50	0.27	5	7.7	20
D45/WB	2.9	1.6	5.5	100	0.08	5	7.1	19
Mean \pm SD	3.6 ± 0.4		5.2 ± 0.2	300 ± 200	0.11 ± 0.07		6.1 ± 1.3	31 ± 9
D20/WB	4.0	6.5	6.0	900	0.02	10	11.3	26
D26/WB	3.6	1.9	5.3	500	0.06	10	7.8	49
D27/WB	3.7	5.6	5.5	500	0.07	10	8.4	41
D32/WB	3.4	12.7	5.3	300	0.06	10	6.4	53
D33/WB	3.6	2.2	5.5	400	0.05	10	6.0	51
D37/WB	3.7	2.5	5.0	200	0.06	10	6.4	34
D41/WB	3.8	5.2	5.5	500	0.07	10	7.2	35
Mean \pm SD	3.7 ± 0.2		5.4 ± 0.3	490 ± 230	0.06 ± 0.02		7.6 ± 0.3	41 ± 10

lower frequencies. As expected, the shift of the cofield peak to lower frequencies increased with increasing DPA concentration in the bathing medium (Table 2).

For extraction of quantitative data for the dielectric properties of plasma membranes from the rotational spectra, the cells are usually modeled as single- or multilayered, nondispersive particles (*see* Eqs. 1, 3, 5 and 6). In the absence of mobile charges (or lipophilic ions) this approach is apparently adequate as shown for the untreated erythrocytes (Fig. 4). Erythrocyte membranes are ideal objects because the area-specific concentration of the electrogenic $\text{N}^+\text{-K}^+\text{-ATPase}$ is very low (400 per cell, *see* Glaser, 1996) and the Cl^- -transporter (correlated with the band 3 protein) is electrically silent. Their contribution to the electric properties of the membrane should, therefore, be very small (Donath & Egger, 1992) as experimentally verified. However, if mobile charges are present, this approach obviously does not have a rigorous theoretical foundation. Mobile charges are common features of many biological membranes and lead (at sufficient high concentrations) to an electric dispersion within the frequency spectrum (Almers, 1978; Lauger et al., 1981). It is, therefore, clear that they must show their imprint in the rotational spectra (Arnold et al., 1985; Arnold & Zimmermann, 1988), although this has

received little attention in the literature. The rotational experiments with erythrocytes pretreated with lipophilic anion and the theoretical considerations developed here illuminate the significance of integration of these transport properties of biomembranes into the current single- and multiple-shell models. Despite some (reasonable) simplifications (Eqs. 8 and 9) of the original equations derived by Lauger and colleagues (Ketterer et al., 1971; Lauger et al., 1981) for the capacitive and conductive increments of the mobile charges, persuasive agreement between theory and experiment had been obtained (Fig. 3 and 6). The values deduced for the translocation rate of the incorporated DPA molecules (Table 2) are of the same order of magnitude as published in the literature for DPA-doped nerve cells (about $12 \times 10^3 \text{ sec}^{-1}$; Benz & Nonner 1981; Benz et al., 1984) and for solvent-free, DPA-doped planar lipid bilayer membranes (about $30 \times 10^3 \text{ sec}^{-1}$, Dilger & Benz, 1985).³ Accordingly, the av-

³ Lipid bilayer membranes made in decane have a much lower value (about 10^3 sec^{-1} , Benz & Zimmermann, 1983), whereas for monoolein bilayers made with the polar solvents 1-chlorodecane or 1-bromodecane the translocations rates of DPA are extremely high (about $30 \times 10^3 \text{ s}^{-1}$; Dilger & Benz, 1985). This shows that the translocation rate of

erage area-specific concentration of DPA within the erythrocyte membrane ($3\text{--}7\text{ nmol m}^{-2}$) agrees well with the equilibrium values of these probe molecules published in the literature mentioned above.

The results reported here have also demonstrated that the signature of the mobile charges is only seen in the rotational spectrum if the external conductivity is adjusted to an appropriate value (see Figs. 1 and 3). The theoretical (Fig. 3) and experimental rotational spectra (Fig. 6) have shown clearly that the electric properties of the mobile charges can be separated experimentally from those of the plasma membrane, provided that the external conductivity did not exceed a certain value. This restricts the exploitation of the electrorotation method at the present to relatively low-conductivity solutions, although future work on cells using other artificial mobile charges or on (genetically manipulated) cells containing natural mobile charges may lead to other conclusions. In any case, improved resolution of the rotation apparatus is required to overcome these limitations. Recent developments in semiconductor technology have shown (see review article of Fuhr et al., 1996), that the developments are not yet at an end and that microstructural electrodes open up new avenues in this field.

Finally, it is worthwhile to note that the theoretical considerations and experimental findings reported here have also an enormous impact on the analysis of cell dielectrophoresis spectra. Because dielectrophoresis and rotational spectra are intimately related (see Eq. 1), theoretical treatment of dielectrophoresis spectra demands a similar expansion of interpretation and the extensive literature published in this field must be obviously reinterpreted to some extent (see Jones, 1995; Fuhr et al., 1996).

We are very grateful to Ms. K. Hämel and Ms. E. Horn for skillful technical assistance. This work was supported by grants of the Deutsche Forschungsgemeinschaft (SFB 176, project B5) and of the Bundesministerium für Bildung, Wissenschaft, Forschung und Technologie (VDI 13 MV 0305) to U.Z.

References

- Almers, W. 1978. Gating currents and charge movements in excitable membranes. *Rev. Physiol. Biochim. Pharmacol.* **82**:96–190
- Arnold, W.M., Wendt, B., Zimmermann, U., Korenstein, R. 1985. Rotation of a single swollen thylakoid vesicle in a rotating electric field. Electrical properties of the photosynthetic membrane and their modification by ionophores, lipophilic ions and pH. *Biochim. Biophys. Acta* **813**:117–131
- Arnold, W.M., Zimmermann, U. 1982. Rotating-field-induced rotation and measurement of the membrane capacitance of single mesophyll cells of *Avena sativa*. *Z. Naturforsch.* **37c**:908–915
- Arnold, W.M., Zimmermann, U. 1983. Patent application, official designation P3325 843.0, received at the Patent Office, FRG, July 18, 1983
- Arnold, W.M., Zimmermann, U. 1988. Electro-rotation: development of a technique for dielectric measurements on individual cells and particles. *J. Electrostatics* **21**:151–191
- Arnold, W.M., Zimmermann, U. 1989. Measurements of dielectric properties of single cells or other particles using direct observation of electro-rotation. In: Proceedings of The First International Conference on Low Cost Experiments in Biophysics, Cairo, 18–20 December, 1989. pp. 1–13
- Arnold, W.M., Zimmermann, U., Heiden, W., Ahlers, J. 1988. The influence of tetraphenylborates (hydrophobic anions) on yeast cell electro-rotation. *Biochim. Biophys. Acta* **942**:96–106
- Becker, F.F., Wang, X.-B., Huang, Y., Pethig R., Vykoukal, J., Gascoyne, P.R.C. 1995. Separation of human breast cancer cells from blood by differential dielectric affinity. *Proc. Natl. Acad. Sci. USA* **92**:860–864
- Benz, R., Conti, F. 1981. Structure of the squid axon membrane as derived from charge-pulse relaxation studies in the presence of absorbed lipophilic ions. *J. Membrane Biol.* **59**:91–104
- Benz, R., Conti, F., Fioravanti, R. 1984. Extrinsic charge movement in the squid axon membrane. Effect of pressure and temperature. *Eur. Biophys. J.* **11**:51–59
- Benz, R., Läger P. 1977. Transport kinetics of dipicrylamine through lipid bilayer membranes. Effects of membrane structure. *Biochim. Biophys. Acta* **468**:245–258
- Benz, R., Läger, P., Janko, K. 1976. Transport kinetics of hydrophobic ions in lipid bilayer membranes. Charge-pulse relaxation studies. *Biochim. Biophys. Acta* **455**:701–720
- Benz, R., Nonner, W. 1981. Structure of the axolemma of frog myelinated nerve: relaxation experiments with lipophilic probe ion. *J. Membrane Biol.* **59**:127–134
- Benz, R., Zimmermann, U. 1983. Evidence for the presence of mobile charges in the cell membrane of *Valonia utricularis*. *Biophys. J.* **43**:13–26
- Dilger, J.P., Benz, R. 1985. Optical and electrical properties of thin monoolein lipid bilayers. *J. Membrane Biol.* **85**:181–189
- Donath, E., Egger M. 1992. Oscillating electric fields as possible probes for studying fast ion exchange. In: Progress in Cell Research, Vol. 2. E. Bamberg and H. Passow, editors. pp. 169–172. Elsevier Science, Amsterdam
- Donlon, J.A., Rothstein, A. 1969. The cation permeability of erythrocytes in low ionic strength media of various tonicities. *J. Membrane Biol.* **1**:37–52
- Engel, J., Donath, E., Gimsa, J. 1988. Electrorotation of red cells after electroporation. *Studia biophysica* **125**:53–62
- Fernandez, J.M., Taylor, R.E., Bezanilla, F. 1983. Induced capacitance in the squid giant axon. *J. Gen. Physiol.* **82**:331–346
- Fuhr, G., Zimmermann, U., Shirley, S.G. 1996. Cell motion in time-varying fields: Principles and potential. In: Electromanipulation of Cells. U. Zimmermann and G.A. Neil, editors. pp. 259–328. CRC Press, Boca Raton, Florida
- Gascoyne, P.R.C., Becker, F.F., Wang, X.-B. 1995. Numerical analysis of the influence of experimental conditions on the accuracy of dielectric parameters derived from electrorotation measurements. *Bioelectrochem. Bioenergetics* **36**:115–125
- Gimsa, J., Schnelle, Th., Zechel, G., Glaser, R. 1994. Dielectric spectroscopy of human erythrocytes: investigation under the influence of nystatin. *Biophys. J.* **66**:1244–1253
- Glaser, R. 1996. Electric properties of the membrane and the cell

these probe molecules depends strongly on the thickness, the dielectric constant of the lipid component and other structural features of the membrane (Benz & Conti, 1981; Benz & Nonner, 1981; Fernandez, Taylor & Bezanilla, 1983).

- surface. In: Electromanipulation of Cells. U. Zimmermann and G.A. Neil, editors. pp.329–363. CRC Press, Boca Raton, Florida
- Jones, T.B. 1995. Electromechanics of Particles. Cambridge University Press, New York
- Ketterer, B., Neumcke, B., Luger, P. 1971. Transport mechanism of hydrophobic ions through lipid bilayer membranes. *J. Membrane Biol.* **5**:225–245
- Luger, P., Benz, R., Stark, G., Bamberg, E., Jordan, P.C., Fahr, A., Brock, W. 1981. Relaxation studies of ion transport systems in lipid bilayer membranes. *Quarterly Reviews of Biophysics* **14**:513–598
- Pauly, H., Schwan, H.P. 1959. uber die Impedanz einer Suspension von kugelformigen Teilchen mit einer Schale. Ein Modell fur das dielektrische Verhalten von Zellsuspensionen und von Proteinlosungen. *Z. Naturforsch.* **14b**:125–131
- Sukhorukov, V.L., Djuzenova, C.S., Arnold, W.M., Zimmermann, U. 1994. DNA, protein and plasma-membrane incorporation by arrested mammalian cells. *J. Membrane Biol.* **142**:77–92
- Sukhorukov, V.L., Djuzenova, C.S., Frank, H., Arnold, W.M., Zimmermann, U. 1995. Electroporabilization and fluorescent tracer exchange: the role of whole cell capacitance. *Cytometry* **21**:230–240
- Sukhorukov, V.L., Arnold, W.M., Zimmermann, U. 1993. Hypotonicity induced changes in the plasma membrane of cultured mammalian cells. *J. Membrane Biol.* **132**:27–40
- Wang, J., Sukhorukov, V.L., Djuzenova, C.S., Zimmermann, U. 1996. Protoplasts of the giant marine alga *Valonia utricularis*: electrical and membrane transport properties measured by electrorotation. *Protoplasma* (in preparation)
- Wang, J., Wehner, G., Zimmermann, U., Benz, R. 1991. Influence of external chloride concentration on the kinetics of mobile charges in the cell membrane of *Valonia utricularis*. *Biophys. J.* **59**:235–248
- Wang, J., Zimmermann, U., Benz, R. 1994. Contribution of electrogenic ion transport to impedance of the algae *Valonia utricularis* and artificial membranes. *Biophys. J.* **67**:1582–1593
- Wolfram, S. 1991. Mathematica. A system for Doing Mathematics by Computer. 2nd Edition. Addison-Wesley, Redwood City, California
- Wulf, J., Benz, R., Pohl, G.W. 1977. Properties of bilayer membranes in the presence of dipicrylamine. A comparative study by optical absorption and electrical relaxation measurements. *Biochim. Biophys. Acta* **465**:429–442
- Zimmermann, U., Buchner, K.-H., Benz, R. 1982. Transport properties of mobile charges in algal membranes: influence of pH and turgor pressure. *J. Membrane Biol.* **67**:183–197